Catalytic Performance of H_3PO_4-Modified Cerium Oxide as Catalyst for Ethylene Production from Ethanol Dehydration

SooLing Chong, JiahChee Soh and ChinKui Cheng

***Abstract*—**Production of ethylene from ethanol dehydration was investigated over H_3PO_4 (10wt% to 30wt%)-modified cerium oxide catalysts synthesized by wet impregnation technique. The physicochemical properties of the fresh catalysts of cerium oxide and H_3PO_4-modified cerium oxide were investigated using N_2 adsorption-desorption, SEM, FTIR, NH3-TPD and XRD. The ethanol catalytic dehydration was carried out in a fixed-bed reactor at 673-773 K and at ethanol partial pressure of 33 kPa. The effects of phosphorus loading on catalyst and reaction temperatures were investigated in terms of catalytic activity towards conversion and product selectivity. Overall, the selectivity of ethylene increased with the temperature and phosphorus loading. The highest ethylene selectivity and ethanol conversion were 99% and 60%, respectively, at 773 K and 33 kPa over the 30wt% H_3PO_4-modified cerium oxide.

***Keywords*—** ethylene production, ethanol dehydration, H3PO4 modification, cerium oxide

I. Introduction

The increasing demand of ethylene is due to its uses in producing polyethylene, one of the primary components in the most of the plastic and in petrochemical industry [1]. Besides that, ethylene acts as precursors for surfactant chemicals such as ethylene oxide or ethylene glycol. With increased demand, global ethylene production has grown at an average rate of almost 4.5% per year from 2009-2014. Currently steam cracking of hydrocarbon from fossil fuel is still dominating the production market because of the high production cost and energy consumption associated with catalytic dehydration pathway. Due to the increasing demands for energy, stricter environmental regulations, and continued depletion of fossil feedstock, alternative and renewable energy resources have attracted increased interest in recent research. In the view of potential limitations of ethylene availability from the current sources, catalytic dehydration of ethanol (especially bioethanol) to ethylene has become a completely renewable process for producing ethylene [2].

Ethanol dehydration is a process in which water molecules are removed, or the equivalent of water molecules removed from ethanol to produce ethylene when heated together with catalyst. There are two reactions that occur in parallel during catalytic dehydration of ethanol as in Eqns. (1) to (2):

$$C_2H_5OH \leftrightarrow C_2H_4+H_2O \qquad +44.9\text{kJ/mol} \quad (1)$$

$$2C_2H_5OH \leftrightarrow C_2H_5OC_2H_5 + H_2O \qquad -25.1 \text{ kJ/mol} \quad (2)$$

The low temperature favours the side reaction to produce diethyl ether; in contrast, higher reaction temperature is theoretically favouring the main reaction (ethanol dehydration). The dehydration reaction is endothermic and need 390 calories per gram of ethylene produced. The temperature of diethyl ether formation is mainly between 423 K and 573 K, while ethylene formation is favoured between 593 K and 773 K.

Acidic catalysts are often used in ethylene production from ethanol dehydration. The traditional homogeneous catalysts used are sulphuric acid or phosphoric acid in almost all industrial scale processes. The former usually requires higher reaction temperatures and yields lower ethylene selectivity [3]. Due to the low yield and byproducts formation, sulphuric acid and phosphoric acid have been replaced by heterogeneous catalysts such as alumina.

Many studies have been carried out with different technologies and using various acidic heterogeneous catalysts such as alumina, silica, zeolites, metal oxides and heteropolyacids [4]–[6]. Among those studied catalysts, gamma alumina (γ-Al2O3) and HZSM-5 zeolite have drawn the most attention for their high activity and selectivity. HZSM-5 has been widely used in alcohol

SooLing Chong
Faculty of Chemical & Natural Resources Engineering
JiahChee Soh
Centre of Excellence for Advanced Research in Fluid Flow
ChinKui Cheng
Universiti Malaysia Pahang, Lebuhraya Tun Razak, 26300
Gambang Kuantan, Pahang, Malaysia
chinkui@ump.edu.my

dehydration reactions due to its uniform pore structure, high surface area, and adjustable acidity. Low reaction temperature (>473 K) favours the reaction towards ethylene production from ethanol dehydration over HZSM-5. HZSM-5 can achieve 60-80% ethylene yield at relatively low reaction temperature (473-573 K) [7]. Besides of the reaction temperature, the catalyst surface acidity is a significant catalytic performance factor. HZSM-5 has high concentration of strong acidic sites, which exist at low Si/Al ratios helps in ethylene production. However, the high acidity also leads to render HZSM-5 zeolite unstable and low anti-coking property [8]. On the contrary, γ-Al2O3 has high surface area (50-300 m2 g-1) and thermal stability up to 873 K that make it widely used in industrial. The ethanol dehydrate over γ-Al2O3 can achieve greater than 90% to form ethylene. The disadvantage of γ-Al2O3 is high reaction temperature needed for ethanol catalytic dehydration. Another problem is that water can deactivate active sites on γ-Al2O3 and inhibit the formation rate of ethylene and diethyl ether [9].

The weak acid centers and relatively strong acid centers of the catalyst are the active sites of ethanol intramolecular dehydration to ethylene [5]. However, the strong acid centers can easily lead to ethylene polymerization. Hence, surface acidity of catalyst need to adjust using additives to improve catalyst stability and high ethylene selectivity. In continuation of discovering new catalyst for ethanol catalytic dehydration, we report the use of ceria-based catalysts for the aforementioned reaction. The use of cerium oxide as a support offers advantages such as its high oxygen mobility associated with oxygen vacancies and oxygen storage capacity. Due to the high effectiveness of cerium oxide as a support (and the phosphoric acid), many studies have been carried out by employing cerium oxide as catalyst for ethanol conversion reactions especially steam reforming reactions [10]–[13]. As mentioned earlier, the surface acidity of catalyst is important in this reaction. Thus, pure CeO_2 as well as phosphoric acid (H_3PO_4) doped CeO_2 catalysts were prepared to investigate the behaviour of CeO_2 towards kinetics of ethanol dehydration.

Therefore, the aim of this study is to study the feasibility of ethanol dehydration over H_3PO_4-modified cerium oxide catalysts. The synthesized catalysts were characterized using SEM, N_2 adsorption-desorption method, XRD, FTIR and NH_3-TPD for the physicochemical properties.

II. Experimental

A. Catalyst Preparation

Cerium nitrate salt Ce(NO3)2 was procured from Sigma-Aldrich, USA. The ceria support was prepared by thermal decomposition of Ce(NO3)2.6H2O at 873 K for 2 h and then crushed to powder. The modified cerium oxide phosphate catalyst (10PA-CeO2) was prepared by impregnating the 10wt% aqueous solution of H3PO4 into 90wt% of the ceria support followed immediately by magnetic stirring for 3 h. The solution was then magnetic-stirred for 3 h under ambient condition. Thereafter, the impregnated catalyst was oven-dried for 12 h at 373 K. During the first 6 h of the drying process, the catalyst was manually stirred using a glass rod for each hour to maintain relative homogeneity of the slurry. Post 12 h, the calcination of the dried catalyst was carried out in a muffled furnace model Carbolite RHF1400 for 5 h at 773 K with heating rate of 5 K min-1. The catalyst was then cooled to room temperature and ground for physicochemical characterization and reaction studies. The resulting 20PA-CeO2 and 30PA-CeO2 were prepared by the similar procedure with 20wt% and 30wt% of phosphoric acid, respectively.

B. Catalyst Characterization

The phase structure of the catalysts was characterized by X-ray diffraction (Rigaku Miniflex II instrument) using X-ray source from CuKα (λ=1.542 Å) at 30 kV and 15 mA. N2 physisorption was conducted to determine the textural property of the synthesized catalysts. The information about the surface morphology of the catalyst was determined using SEM analysis employing Hitachi TM3030Plus with a magnification of 5 kX. Fourier Transform Infrared Spectroscopy (FTIR) (Perkin Elmer Spectrum 100) was also employed to determine the nature of chemical bonding of the catalysts. Ammonia temperature-programmed desorption (NH3-TPD) was carried out in a Thermo Finnigan TPDRO 1100 to determine the acid properties of fresh catalysts.

C. Catalytic Activity

The reaction was conducted in a fixed-bed reactor at ethanol partial pressure of 33 kPa with WHSV of 240 h-1, in the temperature range of 673-773K. The reactor was loaded with 0.3 g of catalyst and pure ethanol (≥99.9%) was introduced to the reactor with a HPLC pump. The gaseous products were collected and identified using GC to identify the quantity of targeted product. The GC instrument used was Shimadzu GC-2014 with two packed column, column temperature and flame ionizer detector temperature at 333 K and 473 K, respectively. Ethanol conversion and products selectivity were calculated by Eqns. (3) and (4):

$$X_{ethanol} = \frac{\Sigma F_{Pi}}{2 \times F_{ethanol\ in}} \times 100 \quad (3)$$

$$S_{ethylene} = \frac{F_{ethylene}}{\Sigma F_{Pi}} \times 100 \quad (4)$$

where F = molar flow rate

P = Gas products produced

i = C_1, C_2, C_3, C_4 and C_5 species

III. Results and Discussion

A. Catalyst Characterizations

Fig. 1 illustrates XRD spectra of CeO2 and 10, 20, 30PA-CeO2. Based on Fig. 1, the high intensity peaks recorded at 2θ readings of 28.6°, 33.1°, 47.48° and 56.36°. This indicated that the CeO2's structure maintained well for all modified catalysts. The structure of catalysts became less crystallinity as affected by H3PO4 loading. There are additional small peaks found for 20PA-CeO2 and 30PA-CeO2 at 2θ readings of 21°, 27° and 43° which can be ascribed to CeP2O7 species. CeP2O7 is a crystalline product in which every Ce atom is joined to six oxygen and every P to four oxygen, with a connectivity of four and six. The P atoms are joined in pairs through shared O atom to form P2O74- units, each of it shared its six remaining oxygen with the CeO6 octahedral. The appearance of CeP2O7 is normally occurred when cerium oxide reacted with phosphoric acid at temperature around 623 K to 1073 K. In this case, the modified cerium oxide phosphate catalysts were prepared at 773 K in a furnace which causes the formation of CeP2O7 species [14].

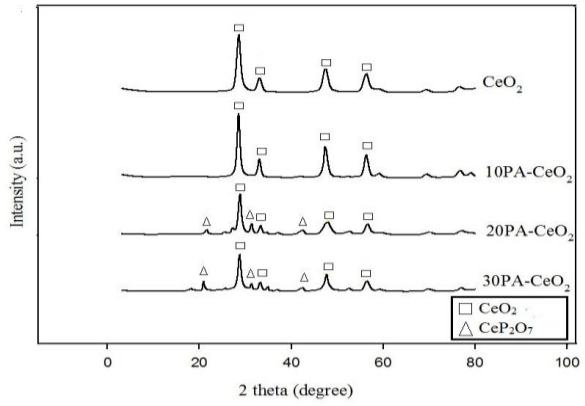

Fig. 1: X-ray diffraction profiles of CeO_2 and H_3PO_4- modified CeO_2 catalysts

SEM micrographs of modified cerium oxide phosphate catalysts at 20 μm resolution are shown in Fig. 2. Based on the Fig. 2, most of the samples were agglomerated together. The SEM images shown in Fig. 2 reveal the morphology of all samples is similar with formation of irregular and bulky surface which is typical of thermally-synthesized wet impregnated catalyst. Meanwhile, it is clearly proved that the addition of H_3PO_4 did not alter the surface morphology of the catalysts.

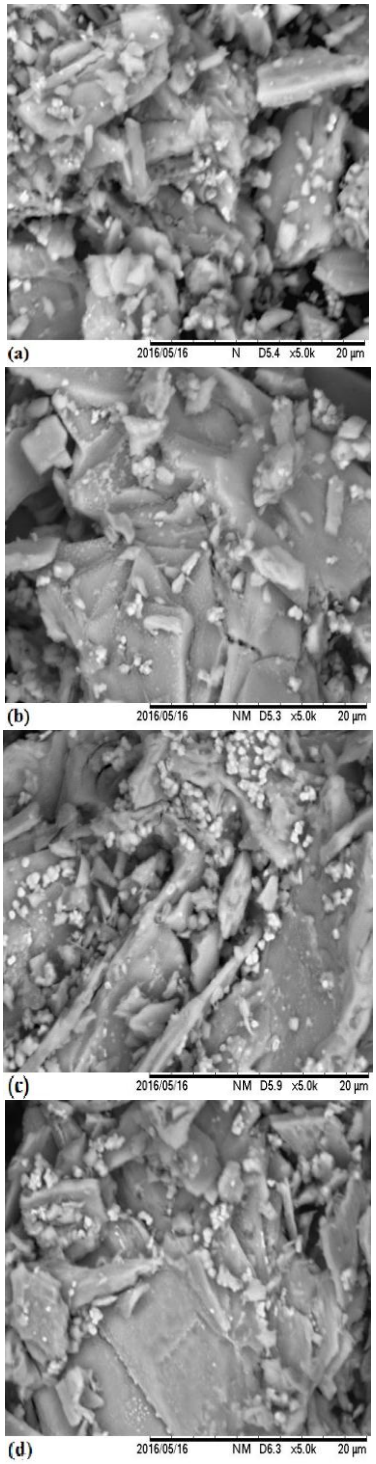

Fig. 2: SEM images of (a) CeO_2, (b) 10PA- CeO_2, (c) 20PA- CeO_2 and (d) 30PA- CeO_2 with magnification of 5*K* obtained from all fresh catalysts

The fresh catalysts were also subjected to the FTIR scanning and the spectra collected are shown in Fig. 3. The spectra were recorded in the wave number that ranged 400-4000 cm^{-1}. Significantly, transmission band representing N-O stretch which normally can be found at wavenumber 3000 cm^{-1} is absent in Fig. 3. This indicates that the entire nitrate group was successfully removed during the thermal decomposition of nitrate-salt to yield pure CeO_2. The

transmission band at wave number 550.73 cm^{-1} represents the Ce-O stretch. In addition, the bands at wavenumber around 900-1000 cm^{-1} represent the O=P=O asymmetric stretching modes of phosphate or polyphosphate species [15]. As shown in Fig. 3, the intense band found around 1000-1600 cm^{-1} increase with the loading of phosphorus. This is due to the introduction of phosphorus onto the CeO_2 catalyst whereby the O=P=O asymmetric stretching increases. The same results observed in previous study [16].

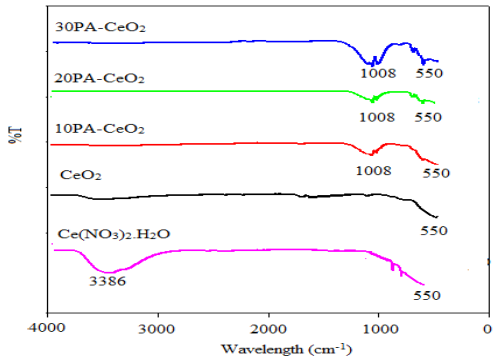

Fig. 3: FTIR result of cerium nitrate, CeO_2 and H_3PO_4-modified CeO_2 catalysts

Table 1 provides the BET specific surface area, mesopore volume and pore diameter of pure CeO_2 and H_3PO_4-modified CeO_2 catalysts that were obtained from N_2 physisorption. Both the BET specific surface area and mesopore volume decreased with H_3PO_4 loading, to the tune of nearly 90% reduction for the 30wt%H_3PO_4 loading. The reduction of pore dimension or pore blockage of the CeO_2 by the introducing of phosphoric acid in the treatment [17]. In contrast, the pore diameter recorded an increment, from 14.0 nm improved to 18.8 nm when the H_3PO_4 weight was increased. This could be due to the creation of wider pore mouth on the surface of CeO_2 resulting from the acid attack that occurred at the employed calcination temperature.

TABLE I:
TEXTURAL PROPERTIES OF THE CEO_2 AND H_3PO_4-MODIFIED CEO_2 CATALYSTS.

Fresh Catalyst	BET Specific Surface Area (m^2 g^{-1})	Pore Volume (cm^3 g^{-1})	Pore Diameter (nm)
CeO_2	71.6	0.2545	14.0
10PA-CeO_2	35.5	0.1461	16.3
20PA-CeO_2	20.2	0.0833	16.3
30PA-CeO_2	9.9	0.0461	18.8

Thermo-desorption profiles of NH3 were carried out to determine the acid properties of the as-synthesized catalysts. The acid strength can be categorized into weak acidic site (373-523 K), moderate acidic site (523-673 K) and strong acidic site (673- 823 K), respectively, based on the desorption temperature. Table 2 shows the resulting acid amount of CeO2 and H3PO4-modified CeO2 catalysts. From Table 2, it can be observed that there are three types of acid sites with variable amounts, at 819 µmol g-1, 188 µmol g-1 and 548 µmol g-1, respectively, for weak, moderate and strong acids found in CeO2 catalyst. The introduction of H3PO4 generates moderate acid sites by suppressing the strong acid sites of CeO2. The amount of moderately-strong acid site has increased substantially, increasing incrementally to 837 µmol g-1 for 10PA- CeO2, 1238 µmol g-1 for 20PA- CeO2 and 1532 µmol g-1 for 30PA- CeO2, respectively. This may be due to the nature of H3PO4, which is a moderately-strong acid with pKa value of 6.9 x 10-3. Moreover, the strong acid site which was inititally present on the surface of pure CeO2 was dimishing with the H3PO4 loading, decreased from 548 µmol g-1 for pure CeO2 to just 284 µmol g-1 for 30PA-CeO2 catalyst. As the loading of phosphoric acid on CeO2 increases, the total acid amount increases.

TABLE II:
THE TOTAL SURFACE ACIDITY AND ACID STRENGTH DISTRIBUTION OF CEO_2 AND H_3PO_4-MODIFIED CEO_2 CATALYSTS

Fresh Catalyst	Acid amount (µmol g^{-1})			Total acid amount (µmol g^{-1})
	Weak acid site (373-523 K)	Moderate acid site (523-673 K)	Strong acid site (673-823 K)	
CeO_2	819	188	548	1555
10PA-CeO_2	850	837	413	2100
20PA-CeO_2	838	1238	385	2461
30PA-CeO_2	823	1532	284	2639

B. Catalyst Peformances of Modified Cerium Oxide Phosphate Catalysts

Fig. 4 shows the product distribution over CeO_2 and 10, 20, 30PA- CeO_2 catalyst at different reaction temperature and ethanol partial pressure 33 kPa. Cerium oxide catalyst presented lowest catalytic performance among all synthesized catalysts. The pure CeO_2 catalyst, under the same reaction condition as aforementioned, the conversions recorded were 1.25%, 2.45% and 6.89%, respectively. This reveals that the acidity amount found in CeO_2 cannot protonate the hydroxyl group of C_2H_5OH which explains its low activity. The selectivity decreases with the increasing reaction temperature. This is due to

higher hydrocarbons formation with almost 35% at 773 K. CeO_2 presents highest number of strong acidic sites which lead to the higher hydrocarbons formation [17], [18]. Hence, there were over 45% of hydrocarbons formed over CeO_2 catalyst at high temperature.

Upon doping with H_3PO_4, the ethylene selectivity and ethanol conversion increase as the loading of H_3PO_4 increase. The addition of H_3PO_4 into CeO_2 catalyst causes the amount of strong acidic sites decrease. This change suppresses the formation of higher hydrocarbons and improves the ethylene production. Although 10PA-CeO_2 did not present a high catalytic performance with low ethanol conversion 4.79%, 8.96% and 29.90% for 673 K, 723 K and 773 K, respectively, but it showed increasing trend in terms of catalytic performance as compared to pure CeO_2. This indicates that the surface acidity of 10PA-CeO_2 was unable to catalyze the formation of products. Among all CeO_2 and H_3PO_4-modified CeO_2 catalysts, the 30PA-CeO_2 catalyst showed the best catalytic performance. On this catalyst, the products are dominated by ethylene under all reaction condition with over 95% of ethylene selectivity. The presence of moderate weak acidic sites in this catalyst helps to suppress the formation of higher hydrocarbons. Besides that, the blockage of pore volume after the addition of H_3PO_4 helps in reducing the multiple adsorptions of ethanol whereby results in the improvement in ethylene selectivity.

In addition, 10, 20 and 30PA-CeO_2 present an increasing trend in both ethanol conversion and ethylene selectivity as the temperature increases. Among all the CeO_2 and H_3PO_4-modified CeO_2 catalysts, 30PA-CeO_2 catalyst showed the best catalytic performance. With increasing reaction temperature, both ethanol conversion and ethylene selectivity increased, *viz.* conversion of ethanol increased from 15.97% at 673 K to 59.74% at 773 K, whilst the ethylene selectivity improved from a low of 96.14% at 673 K to 99% at 773 K. This showed that the dehydration activity of 30PA-CeO_2 catalyst improved with reaction temperature. This indicates that H_3PO_4 functioned more effectively with reaction temperature, *i.e.* its acidity property can be tailored to the reaction temperature and thus, able to protonate the hydroxyl group of C_2H_5OH molecule.

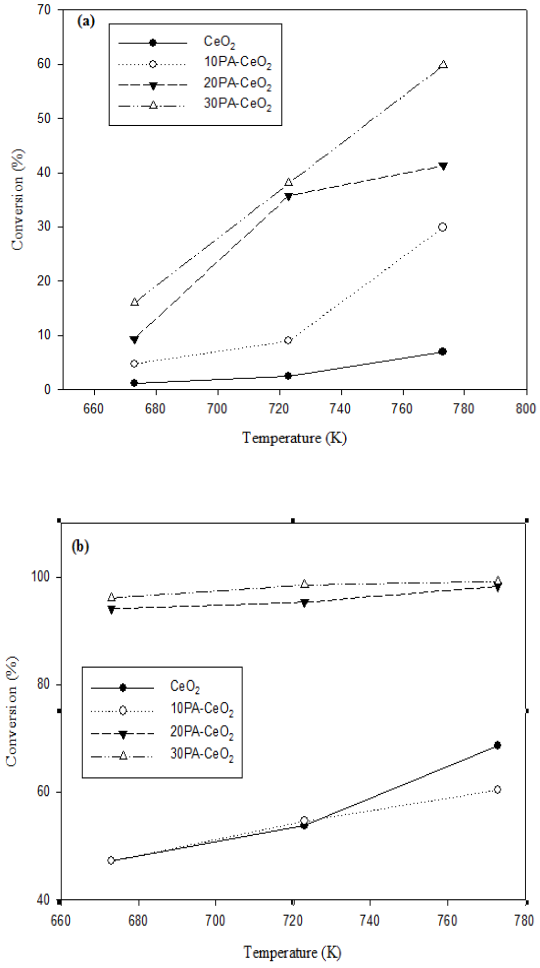

Fig. 4: Catalytic performance (a) ethanol conversion and (b) ethylene selectivity of CeO_2 and H_3PO_4-modified CeO_2 catalysts at 673 to 773K and ethanol partial pressure 33kPa.

IV. Conclusion

This project focuses on the catalytic performance of ethanol to ethylene on H3PO4-modified CeO2 (various loadings of H3PO4) catalysts and the influences of H3PO4 on ethanol conversion over the synthesized catalysts. The addition of phosphoric acid to the CeO2 catalyst improves the catalytic performance and catalyst stability for ethanol dehydration to ethylene. These improvements are due to the tuned acid. The H3PO4-modified CeO2 catalysts showed increasing trend in ethanol conversion and ethylene selectivity with the loading of phosphorus.

Acknowledgment

We thank Universiti Malaysia Pahang for providing UMP Short Term Grant RDU160335 to support this work..

References

[1] A. Morschbacker (2009). Bio-Ethanol Based Ethylene. Polym. Rev. [Online]. 49. pp. 79–84. Available: http://www.tandfonline.com/doi/abs/10.1080/15583720902834791 https://doi.org/10.1080/15583720902834791

[2] I. Takahara, M. Saito, M. Inaba, and K. Murata (December 2005). Dehydration of Ethanol into Ethylene over Solid Acid Catalysts. Catal. Letters. [Online]. 105(3–4). pp. 249–252. Available: http://link.springer.com/article /10.1007/s10562-005-8698-1 https://doi.org/10.1007/s10562-005-8698-1

[3] D. Fan, D.-J. Dai, and H.-S. Wu (December 2012) Ethylene Formation by Catalytic Dehydration of Ethanol with Industrial Considerations. Materials (Basel). [Online]. 6(1). pp. 101–115. Available: http://www.mdpi.com/1996-1944/6/1/101

[4] A. T. Aguayo, A. G. Gayubo, A. Atutxa, B. Valle, and J. Bilbao (Octocber 2005). Regeneration of a HZSM-5 zeolite catalyst deactivated in the transformation of aqueous ethanol into hydrocarbons. Catal. Today. [Online]. 107–108. pp. 410–416. Available: http://www.sciencedirect.com/science/article/pii/S0920586105004529 https://doi.org/10.1016/j.jclepro.2015.09.069

[5] T. K. Phung, L. Proietti Hernández, A. Lagazzo, and G. Busca (March 2015). Dehydration of ethanol over zeolites, silica alumina and alumina: Lewis acidity, Brønsted acidity and confinement effects. Appl. Catal. A Gen. [Online]. 493. pp. 77–89. Available: http://www.sciencedirect.com/science/article/pii/S0926860X14008096 https://doi.org/10.1016/j.apcata.2014.12.047

[6] D. Varisli, T. Dogu, and G. Dogu (Octocber 2007). Ethylene and diethyl-ether production by dehydration reaction of ethanol over different heteropolyacid catalysts. Chem. Eng. Sci. [Online]. 62. pp. 5349–5352. Available: http://www.sciencedirect.com/science/article/pii/S0009250907000681

[7] F. F. Madeira, N. S. Gnep, P. Magnoux, S. Maury, and N. Cadran (Octocber 2009). Ethanol transformation over HFAU, HBEA and HMFI zeolites presenting similar Brønsted acidity. Appl. Catal. A Gen. [Online]. 367(1–2). pp. 39–46. Available: http://www.sciencedirect.com/science/article/pii/S0926860X09005456

[8] N. Zhan, Y. Hu, H. Li, D. Yu, Y. Han, and H. Huang (March 2010). Lanthanum-phosphorous modified HZSM-5 catalysts in dehydration of ethanol to ethylene: A comparative analysis. Catal. Commun. [Online]. vol. 11, no. 7, pp. 633–637. Available: http://www.sciencedirect.com/science/article/pii/S1566736710000130 https://doi.org/10.1016/j.catcom.2010.01.011

[9] J. F. DeWilde, H. Chiang, D. a Hickman, C. R. Ho, and A. Bhan (March 2013). Kinetics and Mechanism of Ethanol Dehydration on γ-Al2O3 : the critical role of dimer inibition. ACS Catal. [Online]. 3(4). pp. 798–807. Available: http://pubs.acs.org/doi/abs/10.1021/cs400051k

[10] W. Cai, F. Wang, E. Zhan, A. C. Van Veen, C. Mirodatos, and W. Shen (July 2008). Hydrogen production from ethanol over Ir/CeO2 catalysts: A comparative study of steam reforming, partial oxidation and oxidative steam reforming. J. Catal. [Online]. 257(1). pp. 96–107. Available: http://wrap.warwick.ac.uk/53766/ https://doi.org/10.1016/j.jcat.2008.04.009

[11] K. Mudiyanselage, I. Al-Shankiti, A. Foulis, J. Llorca, and H. Idriss (December 2016). Reactions of Ethanol over CeO2 and Ru/CeO2 Catalysts," Appl. Catal. B Environ. [Online]. 102(1-2). pp. 94-100. Available: http://www.sciencedirect.com/science/article/pii/S0926337310005187 https://doi.org/10.1016/j.apcatb.2016.03.065

[12] H. Wang, J. Ye, Y. Liu, Y. Li, and Y. Qin (December 2007). Steam reforming of ethanol over Co3O4/CeO2 catalysts prepared by different methods. Catal. Today. [Online]. 129(3–4). pp. 305–312. Available: http://www.sciencedirect.com/science/article/pii/S0920586107005330 https://doi.org/10.1016/j.cattod.2006.10.012

[13] B. Zhang, X. Tang, Y. Li, W. Cai, Y. Xu, and W. Shen (June 2006). Steam reforming of bio-ethanol for the production of hydrogen over ceria-supported Co, Ir and Ni catalysts. Catal. Commun. [Online]. 7(6). pp. 367–372. Available: http:/www.sciencedirect.com/science/article/pii/S1566736705003249 https://doi.org/10.1016/j.catcom.2005.12.014

[14] K. M. White, P. L. Lee, P. J. Chupas, K. W. Chapman, E. A. Payzant, A. C. Jupe, W. A. Bassett, C. S. Zha, and A. P. Wilkinson (2008). Synthesis, symmetry, and physical properties of cerium pyrophosphate. Chem. Mater. [Online]. 20(11). pp. 3728–3734. Available: http:/pubs.acs.org/doi/abs/10.1021/cm702338h https://doi.org/10.1021/cm702338h

[15] T. Armaroli, G. Busca, C. Carlini, M. Giuttari, A. M. Raspolli Galletti, and G. Sbrana (February 2000). Acid sites characterization of niobium phosphate catalysts and their activity in fructose dehydration to 5-hydroxymethyl-2-furaldehyde. J. Mol. Catal. A Chem. [Online]. 151(1). pp. 233–243. Available: http://www.sciencedirect.com/science/article/pii/S1381116999002484 https://doi.org/10.1016/S1381-1169(99)00248-4

[16] R. F. Brandão, R. L. Quirino, V. M. Mello, A. P. Tavares, A. C. Peres, F. Guinhos, J. C. Rubim, and P. A. Z. Suarez (2009). Synthesis, characterization and use of Nb2O5 based catalysts in producing biofuels by transesterification, esterification and pyrolysis. J. Braz. Chem. Soc. [Online]. 20(5). pp. 954–966. Available: http://www.scielo.br/scielo.php?script=sci_arttext&pid=S0103-50532009000500022 https://doi.org/10.1590/s0103-50532009000500022

[17] K. Ramesh, L. M. Hui, Y. F. Han, and A. Borgna (January 2009). Structure and reactivity of phosphorous modified H-ZSM-5 catalysts for ethanol dehydration. Catal. Commun. [Online]. 10(5). pp. 567–571. Available: http://www.sciencedirect.com/science/article/pii/S1566736708004676 https://doi.org/10.1016/j.catcom.2008.10.034

[18] K. Ramesh, C. Jie, Y. F. Han, and A. Borgna (April 2010). Synthesis, characterization, and catalytic activity of phosphorus modified H-ZSM-5 catalysts in selective ethanol dehydration. Ind. Eng. Chem. Res. [Online]. 49(9). pp. 4080–4090. Available: http:/pubs.acs.org/doi/abs/10.1021/ie901666f https://doi.org/10.1021/ie901666f

Estimating Emission Factors of Fifteen Categories of Meats from Thai-Style Barbeque Activities

Saranya Manatsakarn and Nares Chuersuwan

***Abstract*—** This study aims to determine air emission factors from meats grilling activity commonly found in Thailand. The major air pollutants included CO, NOx, SO2, particulate matter (PM10) and two greenhouse gases (CO2 and CH4). Measurements were conducted in a chamber to collect air emission in stack. Eucalyptus charcoal was solely used as the fuel during the grilling of meats. Gases pollutants were analyzed real-time while PM and CH4 were collected and subsequently analyzed in the laboratory. CH4 concentrations were quantified by a Gas Chromatograph while PM concentrations were quantified by gravimetric methods. Each of meat grilling was replicated nine times for the total of 15 types of meats (n = 135 tests). The average emission factors of all meats ranged from 756.49-3,343.91 g/kg of meat for CO, 0.42-3.58 g/kg of meat for NOx, 0.009-0.042 g/kg of meat for PM10, 10,587.62-47,236.79 g/kg of meat for CO2 and 30.39-171.12 g/kg of meat for CH4. SO2 was not detected. Results from this study was intended to provide insight for emission estimates from food stalls found across the country. These emission factors can be used to generate more realistic emission inventories and therefore improve the results of estimate emissions of meat grilling in Thailand.

***Keywords*—** meat grilling, major air pollutants, greenhouse gas, emission factors.

I. Introduction

Meat grilling is commonly found along the urban street food stalls in Thailand. Charcoal meat grilling is a source of anthropogenic greenhouse gas and major air pollutant released into the atmosphere. Cooking emissions are influenced by the fuel used and the food being cooked [1]. During incomplete combustion of charcoal meat grilling emits particulate matters, carbon dioxide (CO2), carbon monoxide (CO), nitrogen oxides (NOx), volatile organic compounds (VOCs), aldehyde, polycyclic aromatic hydrocarbons (PAH), and total hydrocarbons (THC) [2-5]. During charcoal burning air pollutants can be absorbed in food and degrade air quality in the surrounding environment [6]. Regarding these pollutants, their adverse effects on human health are a great of concern, increasing hazard of the nearby people exposed to pollutants with potential health risks [6]. The pollutant emissions from the combustion such as, PM, NOx and CO have contributed substantially to the regional environment pollution problem [7-8] and meat grilling has the potential to produce net global warming especially CO2, the main driving force for the past global climate change [9-11]. However, the emission factors from meat grilling activities in Thailand are not available.

To evaluate the emissions from meat grilling by charcoal, emission factors are normally used to estimate the emissions. These estimations relate to the quantity of pollutants released into the atmosphere by such activities. The emission factor (EF) represents the quantity of a compound emitted per quantity of fuel consumed (g/kg), per kilogram of meat (g/kg meat) or per unit energy. In this context, the objective of this study is to determine emission factors of gases and particulate matters emitted from grilling activities in Thailand.

II. Methodology

All meats were purchased locally from markets in the area, including pork, chicken, fish, squid, shrimp, Thai sausage, Thai sour pork and meatball. Charcoal derived from eucalyptus woods was used exclusively as the solely fuel. Charcoal was also purchased from local production. This study selected meats that were commonly sale or consumed locally. The grilling tests and results were based on wet weight basis.

Combustion testing equipment has been designed and installed in a laboratory at Suranaree University of Technology. The equipment is in the form of an inverted funnel with a cylinder bottom, 1.20 m. in diameter and 0.80 m. in high. From the top of the cylinder, the tower decreases to 0.28 m. in a length of 0.50 m., and is topped with a stack 1.70 m. in height. Surface area of the stack is

Saranya Manatsakarn
Program in Environmental Pollution and Safety, School of Environmental Health
Nares Chuersuwan
Suranaree University of Technology, Nakhon Ratchasima, Thailand